

Electronic Supplementary Information

Oriented Attachment Mechanism of Triangular Ag Nanoplates: A Molecular Dynamics Study

Tonnam Balankura, Tianyu Yan, Omid Jahanmahin, Jenwarin Narukatpichai, Alan Ng, and Kristen A. Fichthorn*

Details of MD Simulations

We use the Metal-Organic Many-Body (MOMB) Force Field to describe interactions in our system. In the MOMB force field, the interaction between Ag atoms is described with the embedded-atom method (EAM)¹, while the PVP and EG molecules are modeled with the CHARMM force field.^{2,3} The CHARMM force field is an all-atom model, which includes both bonded (bond stretching, bond-angle bending, and torsion) and non-bonded electrostatic and van der Waals (vdW) interactions between the organic molecules. Two pairwise potentials, a Morse potential, and Grimme's potential for vdW interactions⁴ are combined to describe the metal-organic interaction. In addition, the metal-organic interaction is augmented with a many-body EAM embedding energy, which contains a one-way electron density contribution from the oxygen in the organic molecules to Ag.

The EAM potential does not describe long-range vdW interactions between Ag atoms in our system. Thus, to capture these interactions, we included a pair-wise term

$$E_{vdW,Ag}(r_{ij}) = -\frac{C_6}{r_{ij}^6}, \quad (S1)$$

where r_{ij} is the distance between Ag atoms i and j in different nanoplates and the C_6 coefficient is taken from the work of Ruiz et al.,⁵ to provide consistency with the MOMB force field.

The MD simulations are performed in the canonical ensemble using the LAMMPS code,⁶ compiled with our MOMB pair style.⁷ The equations of motion are integrated using the velocity-Verlet algorithm with a 1 fs time step and the temperature is controlled using the Nosé-Hoover thermostat. We consider full motion of PVP and solvent molecules, but atoms in the Ag plates are frozen to their equilibrium positions and we consider rigid-body motion of the plates for greater computational efficiency. Although Ag plate OA was experimentally observed at 373-381 K,^{8,9} we ran our vacuum and solution-phase simulations at 900 K and 600 K, respectively, because this improves sampling efficiency by overcoming the prohibitively slow motion of PVP (on the MD time scale) at the experimental temperatures. We also overcome issues with overbinding of PVP to the Ag nanoplates in vacuum by elevating the temperature.¹⁰ The volume of the simulation box is chosen to be large enough to eliminate interactions between the plates and their periodic images. Since there are partial charges on atoms of the organic molecules, the electrostatic interaction is calculated using the Particle Particle Particle Mesh method with a tolerance of 10^{-4} (dimensionless) relative error in forces.

A system of one frozen Ag nanoplate and PVP molecules is equilibrated for 20 ns in the NVT ensemble. The OA simulation systems are created from duplicating the single plate and PVP molecules. For the solution-phase system, EG molecules are added into the two-plate systems and equilibrated for 10 ns while keeping the plates frozen. To ensure that there are sufficient EG molecules added to model a homogeneous solution-phase, we confirm that the EG density in the bulk solution phase matches the density of a bulk EG system at 373 K.

To perform umbrella sampling simulations for computation of the potential of mean force (PMF), the initial pathways of approach are generated by pulling the plates from a state in which they are separated to a state in which they are attached, using a moving harmonic

potential. The initial configurations along the pulling trajectory are segmented into sampling windows, in which the plates gradually proceed from an attached state to a separated state. Between 85 and 100 windows were used to sample the reaction coordinate. In each window, we apply a biasing harmonic potential on the distance between the plate surfaces while running canonical MD simulations. To focus our investigation on side-to-side vs. face-to-face attachment mechanisms, we applied two additional harmonic biases to impede the plates from rotating or sliding over each other. Plate rotation is limited (but not completely prevented) by applying a harmonic bias, such that the dihedral angle between the plate corners of the approaching sides is zero. To limit plates from sliding over each other, we applied a harmonic bias so that the distance collective variable between the approaching surfaces of the plates is zero, in which this distance collective variable is a projection of the distance vector onto the plane that is defined by the axis of the attachment direction. A spring constant value of 100 eV/Å is used for these two additional harmonic biases, which is relatively strong but does not completely restrict the plates from rotating or sliding over each other. The reaction coordinate, denoted as z , is the distance between the touching surfaces of the nanoplates and this is sampled every 100 time steps. From umbrella sampling, we obtain a histogram of the reaction coordinate, which is used to calculate the PMF via umbrella integration.¹¹ The converged profiles of the vacuum and solvated systems are obtained from 5 ns and 3 ns of sampling per window, respectively.

PMF for Nanoplate Aggregation in PVP and Ethylene Glycol

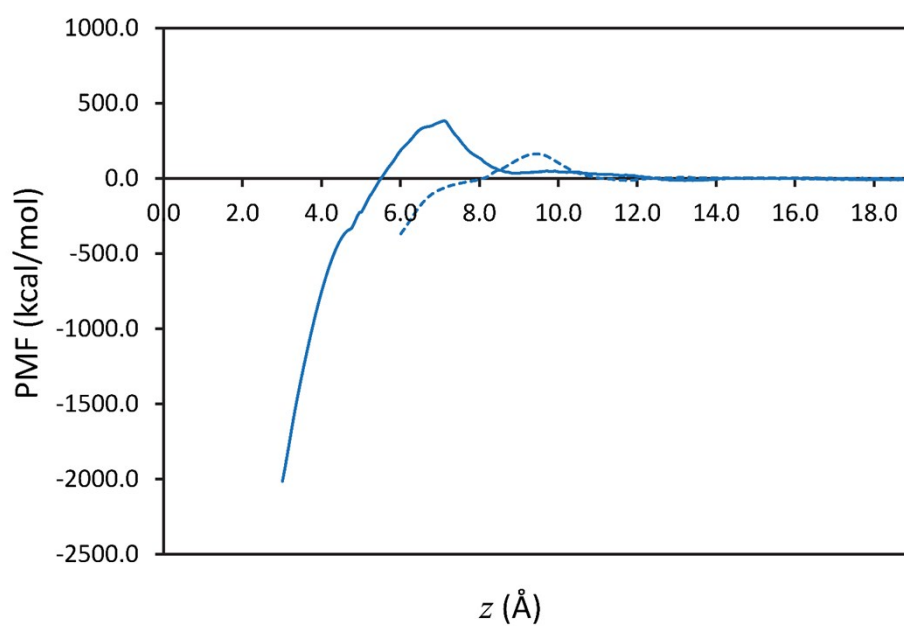


Figure S1. PMF profiles for 148 PVP molecules in EG as a function of the distance between the touching Ag surfaces z . The solid line depicts the face-to-face pathway and the dashed line shows the side-to-side pathway.

Two-Dimensional O-atom Density Map

We obtained two-dimensional (2D) maps of the O-atom density. To obtain these maps, we create 3,600 hexagonal bins in the region above the plane of each facet. The histogram bins are populated by the oxygen atoms that are within 12 Å of the surface. This value is the maximum thickness of the PVP film, obtained from observing the PVP density along the orthogonal direction from each face. We obtain the normalized count of the PVP oxygen atoms that fall within each bin. The counts are normalized by the maximum count of the set of histograms, therefore the normalized count has a range between 0 and 1.

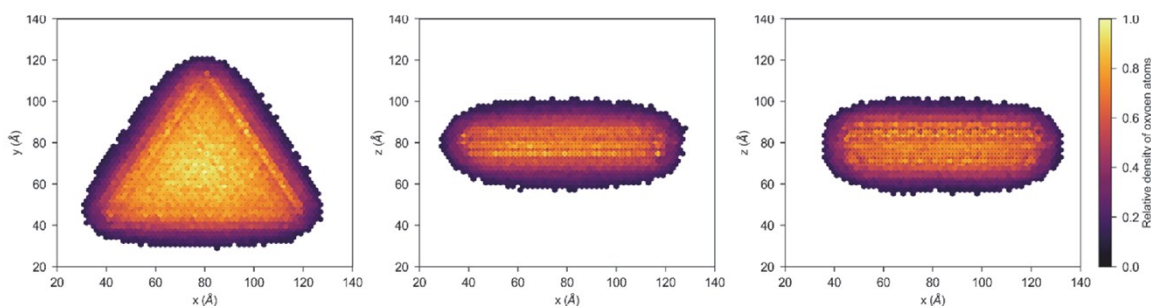


Figure S2. 2D histograms of the PVP oxygen-atom density for a plate with 148 PVP in vacuum. We show densities (going from left to right) for the $\{111\}$ face and two different sides. The black dots denote the Ag surface atoms.

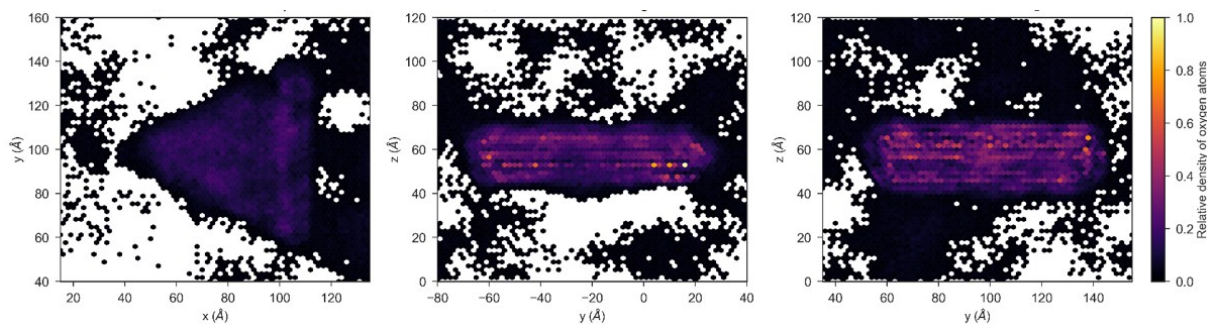


Figure S3. 2D histograms of the PVP oxygen-atom density for a plate with 148 PVP in EG solution. We show densities (going from left to right) for the $\{111\}$ face and two different sides. The black dots denote the Ag surface atoms and the dark regions that extend beyond the plate boundaries represent solution-phase PVP..

References

- 1 J. C. Williams, P. L., Mishin, Y., Hamilton, *Model. Simul. Mater. Sci. Eng.*, 2006, **14**, 817–833.
- 2 I. Vorobyov, V. M. Anisimov, S. Greene, R. M. Venable, A. Moser, R. W. Pastor and A. D. Mackerell, *J. Chem. Theory Comput.*, 2007, **3**, 1120–1133.
- 3 K. Vanommeslaeghe, E. Hatcher, C. Acharya, S. Kundu, S. Zhong, J. Shim, E. Darian, O. Guvench, P. Lopes, I. Vorobyov and A. D. Mackerell, *J. Comput. Chem.*, 2012, **31**, 671–690.
- 4 S. Grimme, *J. Comput. Chem.*, 2006, **27**, 1787–1799.
- 5 V. G. Ruiz, W. Liu, E. Zojer, M. Scheffler and A. Tkatchenko, *Phys. Rev. Lett.*, 2012, **108**, 146108.
- 6 S. Plimpton, *J. Comput. Phys.*, 1995, **117**, 1–19.
- 7 Y. Zhou, W. A. Saidi and K. A. Fichthorn, *J. Phys. Chem. C*, 2014, **118**, 3366–3374.
- 8 Z. Liu, H. Zhou, Y. S. Lim, J. H. Song, L. Piao and S. H. Kim, *Langmuir*, 2012, **28**, 9244–9249.
- 9 M. H. Kim, D. K. Yoon and S. H. Im, *RSC Adv.*, 2015, **5**, 14266–14272.
- 10 T. Balankura, X. Qi and K. A. Fichthorn, *J. Phys. Chem C*, 2018, **122**, 14566–14573.
- 11 J. Kästner and W. Thiel, *J. Chem. Phys.*, 2005, **123**, 144104.